Please cite this article in press as: Gonzalez et al., N-Terminal ArgD Peptides from the Classical *Staphylococcus aureus* Agr System Have Cytotoxic and Proinflammatory Activities, Chemistry & Biology (2014), http://dx.doi.org/10.1016/j.chembiol.2014.09.015

Chemistry & Biology
Brief Communication

N-Terminal ArgD Peptides from the Classical *Staphylococcus aureus* Agr System Have Cytotoxic and Proinflammatory Activities

David J. Gonzalez,[1,2,*] Ross Corriden,[3] Kathryn Akong-Moore,[3] Joshua Olson,[3] Pieter C. Dorrestein,[1,2,4] and Victor Nizet[2,3]
[1]Department of Pharmacology
[2]Skaggs School of Pharmacy and Pharmaceutical Sciences
[3]Department of Pediatrics
[4]Department of Chemistry and Biochemistry
University of California, San Diego, La Jolla, CA 92093, USA
*Correspondence: djgonzalez@ucsd.edu
http://dx.doi.org/10.1016/j.chembiol.2014.09.015

SUMMARY

AgrD is the precursor for the autoinducing peptide in a quorum-sensing system regulating virulence phenotypes of the preeminent pathogen *Staphylococcus aureus*. Mass spectrometry-based methods, including molecular networking, identified formylated and nonformylated peptide variants derived from the AgrD N-terminal leader domain in *S. aureus* cell-free culture supernatants. Functional assessment of these peptides revealed unexpected bioactivities, including human cell-line cytotoxicity, modulation of neutrophil chemotaxis, neutrophil extracellular trap formation, and the aggravation of skin lesions in vivo.

INTRODUCTION

Nearly three decades ago, the accessory gene regulatory (Agr) quorum-sensing system was identified in the leading human bacterial pathogen *Staphylococcus aureus* (Recsei et al., 1986). A classical model of growth phase-dependent gene regulation, Agr is studied for its important role in regulation of surface-expressed or secreted virulence factors. Natural or engineered strains of *S. aureus* with inactivating mutations in *agr* genes lose virulence in animal infection (Abdelnour et al., 1993; Villaruz et al., 2009). Thus, *S. aureus* infectivity depends upon an array of Agr-regulated gene products working in concert to circumvent host innate immune clearance (Novick et al., 1993; Pragman and Schlievert, 2004), yet many mechanistic details of the Agr system remain a mystery.

Agr quorum-sensing dynamics are governed by the posttranslationally modified, thiolactone-containing autoinducing peptide (AIP) (Enright et al., 2002). Genetically, *agr* is composed of two promoters, P2 and P3, which direct the divergent transcription of RNAII and RNAIII according to AIP concentrations. RNAII encodes the four-gene operon *agrABCD*, and within the cluster, AgrB+AgrD and AgrA+AgrC work together to carry out biosynthesis and regulatory functions. AgrD, the AIP precursor substrate, is cleaved and cyclized through thiolactone formation by cell membrane-bound AgrB. AgrA and AgrC combine to form a kinase-dependent two-component regulatory system. During critical regulatory states, the mature AIP binds extracellularly to the AgrC protein kinase, triggering activation of *agrA* and successive induction of divergently expressed promoters P2 and P3. RNAIII expression leads to production of two molecules, the primary effector RNA regulator and delta-toxin or phenol-soluble modulin (PSM) γ, a wide-spectrum cytolysin that is released extracellularly with a formylated initiator methionine, with a nonformylated methionine, or in truncated forms (Gonzalez et al., 2012). Taxonomically, *S. aureus* isolates can be divided into four *agr* groups on the basis of polymorphisms within the *agrABCD* operon (Wright et al., 2005).

Downstream contributions of the mature AIP on *S. aureus* pathogenesis have been the focus of several studies (Harraghy et al., 2007). More recently, reports described the biochemistry of each individual gene product and the relationship between the enzyme AgrB and its substrate AgrD (Thoendel and Horswill, 2009). It is thought that formation of the AIP is initiated by migration of AgrD and its association with the intracellular membrane. The amphipathic AIP N-terminal region contains essential amino acids that stabilize the propeptide, allowing association of core and C-terminal amino acids with AgrB. Endopeptidase AgrB then cleaves the highly conserved C-terminal tail of AgrD to catalyze the formation of a thiolactone ring within the core amino acids. Thereafter, through an unknown mechanism, the AIP precursor is transported across the cell membrane. Once extracellular, the type I signal peptidase SpsB (Kavanaugh et al., 2007) catalyzes the formation of two extracellular final products: (1) AIP and (2) N-terminal peptide (Figure 1A).

Using molecular networking (Watrous et al., 2012), we examined mass spectrometry (MS) data derived from cell-free culture extracts of a representative community-associated methicillin-resistant *S. aureus* (MRSA) USA300 isolate (Kennedy et al., 2010). Analysis of the molecular network revealed extracellular AgrD N-terminal (termed N-AgrD) formylated and truncated peptide variants. Here we show these N-AgrD variant peptides have immunostimulatory properties toward neutrophils isolated from human blood, display broad-spectrum cytotoxicity, and aggravate skin lesion formation caused by Agr-deficient *S. aureus*. This study provides insight into endogenous biosynthetic and virulence properties of the Agr quorum-sensing system, while

Please cite this article in press as: Gonzalez et al., N-Terminal ArgD Peptides from the Classical *Staphylococcus aureus* Agr System Have Cytotoxic and Proinflammatory Activities, Chemistry & Biology (2014), http://dx.doi.org/10.1016/j.chembiol.2014.09.015

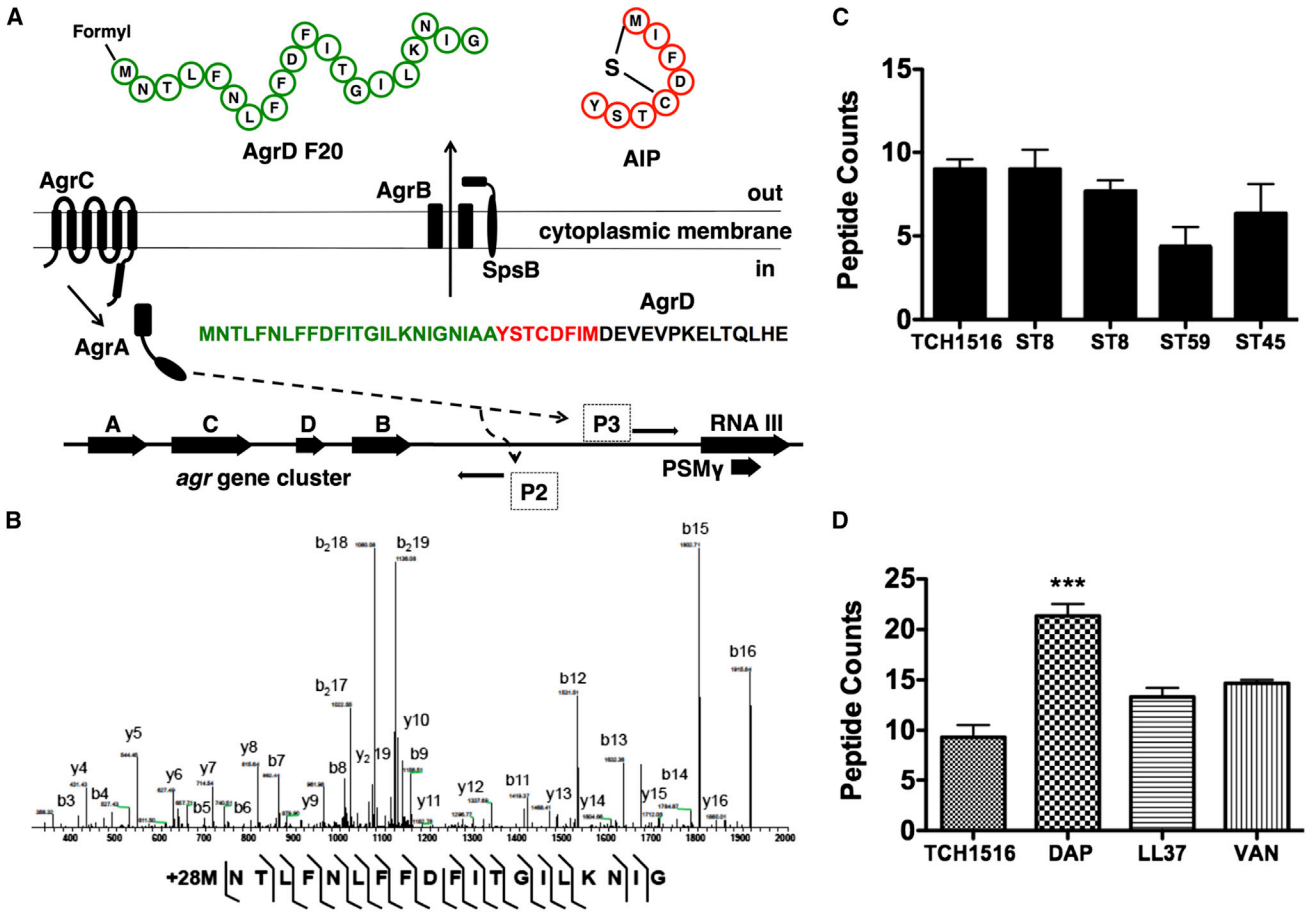

Figure 1. The Accessory Gene Regulatory System and N-AgrD Peptide Properties

(A) Four genes, *agrABCD*, comprise the *agr* biosynthetic network. *agrD* encodes the peptide substrate undergoes posttranslational modification (PTM) by membrane-bound endopeptidase *agrB* through cleavage and thiolactone cyclization. Once extracellular, the hybrid molecule consisting of the AIP and the N-terminal region of AgrD is further processed by peptidase SpsB into mature AIP and N-AgrD. Induction of promoter 2 drives the transcription of the *agr*ABCD operon. Promoter 3 induction results in the expression of RNAIII that produces two final products, the primary RNA effector molecule and PSMγ.

(B) MS survey of several *S. aureus* clinical isolates show detectable N-AgrD peptides as peptide counts.

(C) Tandem MS sequencing of AgrD F24. Several contingent ion fragments, including reliable mass accuracy, localize a PTM of +28 Da to the initiator methionine of N-AgrD.

(D) Antibiotic effects on the number of N-AgrD peptide counts. Challenge with a subinhibitory concentration of daptomycin increased the number of detectable peptides.

Statistical analysis performed by one-way ANOVA; ***$p < 0.001$. Data are expressed as mean ± SD.

revealing functional properties of AgrD beyond its AIP-encoding domain. Furthermore, we highlight the power of the molecular networking platform as a tool to discover unforeseen bioactive peptides within a long-studied, highly important regulatory system of staphylococcal virulence.

RESULTS

Discovery of N-AgrD Variant Peptides by MS-Based Molecular Networking

Molecular networking is an emerging platform based on the concept of mass spectral pairing, which allows the structural grouping and successive mapping of MS data sets. Recently, our group used the platform to build a molecular network representative of extracellularly released, small molecular weight biosynthetic factors produced by MRSA (Gonzalez et al., 2014). Here, we report the continued examination of the created molecular network by de novo sequencing and peptidogenomic approaches (Kersten et al., 2011), recovering peptides pertaining to the AgrD N-terminal domain (Figure S1 available online). Investigation into the identity of each individual mass spectrum within the AgrD grouped family-produced peptide sequence tags corresponding to N-terminal variants with mass offsets of +28 Da, a signature for formyl-methionine modification. With the recovered chemical knowledge from the molecular networks, we used tandem MS data processing program InsPecT (Tanner et al., 2005) to support the de novo sequencing and peptidogenomics identifications. Careful manual annotation of the identified N-AgrD peptides further validated the identifications (Figure 1B; Figures S2–S6). To broaden our survey, we analyzed

Please cite this article in press as: Gonzalez et al., N-Terminal ArgD Peptides from the Classical *Staphylococcus aureus* Agr System Have Cytotoxic and Proinflammatory Activities, Chemistry & Biology (2014), http://dx.doi.org/10.1016/j.chembiol.2014.09.015

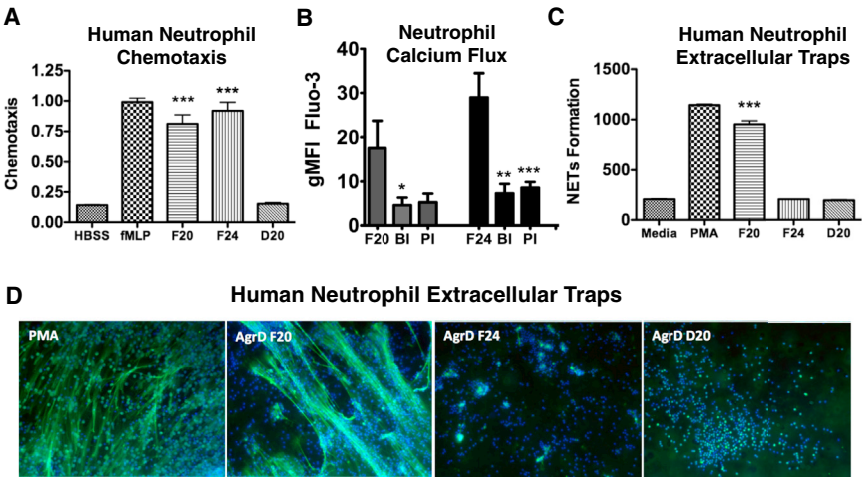

Figure 2. N-AgrD Peptide Variants Stimulate Polymorphonuclear Neutrophil Chemotaxis and NET Formation

(A) As an indicator of migration, elastase enzymatic activity in neutrophil supernatants was measured at 405 nm. Formylated peptides N-AgrD F20 and N-AgrD F24 stimulated increased chemotaxis. The N-AgrD D20 peptide, which is nonformylated, did not exhibit chemoattractant properties.

(B) PMN calcium influx indicating receptor activation. A significant decrease in activation was observed by each pharmacological blockade, indicating that the N-AgrD peptide family functions though a formyl peptide receptor-dependent mechanism. BI, BOC, a selective inhibitor of FPR1; PI, PBP, a selective inhibitor of FPR2.

(C) The Quant-iT Picogreen assay was used to quantify extracellular DNA release upon stimulation by the N-AgrD peptides. Only formylated peptide N-AgrD F20 stimulated a significant increase in NET production.

(D) Microscopy confirmed only peptide N-AgrD D20 stimulated formation of web-like DNA structures similar to the phorbol myristate acetate positive control.

Statistical analysis by one-way ANOVA; ***$p < 0.001$. Data are expressed as mean ± SD.

cell-free culture extracts of 12 additional *S. aureus* strains or clinical isolates (Table S1). N-AgrD peptides were produced by three USA300 lineage MRSA, two ST59 MRSA (Huang et al., 2012), and clonal colony ST45 of USA600 MRSA lineage (Figure 1C). In successive MS experiments, peptide sequences most abundantly mapped to AgrD (McIlwain et al., 2012), herein designated (1) N-AgrD F20, (2) N-AgrD F24, and (3) N-AgrD D20, were synthesized and isolated at >95% purity for functional assessment.

Properties of the N-AgrD Variant Peptides

To estimate the production and release of the N-AgrD variants, MRSA USA300 cell-free cultures were extracted and examined by tandem MS. N-AgrD peptides were detected only in late exponential phase extracts, in agreement with previous reports on the temporal production of the AIP (Junio et al., 2013). Estimated AIP culture concentrations vary from 2 to 10 μM (Junio et al., 2013); therefore, we predicted that N-AgrD peptide variants would be detected in stoichiometric concentrations. We detected 2 to 3 μM N-AgrD F24 in extracted cultures of USA300 strain TCH1516 and 1 to 2 μM in extracted cultures of the ST59 strain. There was increased abundance of N-AgrD peptides upon exposure of MRSA to subinhibitory concentrations of cell-wall active antibiotics daptomycin (0.125 mg/l) or vancomycin (0.125 mg/l), or human cationic defense peptide LL-37 (1.2 mg/l) (Figure 1D).

Polymorphonuclear Neutrophil Chemotaxis Induced by N-AgrD Formylated Variants

Leukocytes of the host innate immune system recognize formylated bacterial products as pathogen-associated molecular patterns (Mogensen, 2009), as mediated through formyl peptide receptors (FPR), a class of G protein-coupled receptors associated with chemotaxis. The human FPR family is composed of three members, FPR1, FPR2/ALX, and FPR3; only the first two are expressed in neutrophils. Recently, members of the *S. aureus*-derived phenol-soluble modulin (PSM) peptide family were shown to selectively activate FPR2/ALX (Kretschmer et al., 2010). Because N-AgrD F20 and N-AgrD F24 peptides contained formyl groups, we tested their abilities to act as chemoattractants for human neutrophils. Nanomolar quantities of N-AgrD F20, N-AgrD F24, and N-AgrD D20 were placed in a chamber adjacent to a suspension of freshly isolated neutrophils, and chemotaxis was quantified. Both formylated peptides N-AgrD F20 and F24 showed strong chemoattractant properties comparable with the well-known chemoattractant formyl-methionyl-leucyl-phenylalanine, whereas nonformylated N-AgrD D20 did not stimulate chemotaxis (Figure 2A). Using specific antagonists of the FPR1 and FPR2 receptors and calcium influx as a surrogate measure of receptor activation (Dixit et al., 2012), significant decreases in receptor activation were observed by pharmacological blockade, indicating that the N-AgrD peptides function though a FPR-dependent mechanism (Figure 2B).

NET Induction by the N-AgrD F20 Formylated Peptide

Neutrophil extracellular trap (NET) formation is a specialized cell death process wherein nuclear DNA is extruded to ensnare and kill pathogens (Brinkmann et al., 2004). As quantified by DNA release, AgrD F20 strongly stimulated NET formation (Figure 2C), whereas no stimulatory effects were observed with peptides N-AgrD F24 and N-AgrD D20. N-AgrD F20 stimulation of NETs was corroborated by fluorescence microscopy, which showed the hallmark weblike NET structures were formed by neutrophils upon N-AgrD F20 stimulation (Figure 2D).

N-AgrD Variant Peptides Cytotoxicity against Human Cell Lines and Erythrocytes

Hemolytic ability of the N-AgrD peptides was tested against erythrocytes from freshly washed human blood. N-AgrD F20 and N-AgrD F24 showed significant hemolytic activity, but N-AgrD D20 peptide did not induce erythrocyte lysis (Figure 3A). USA300 MRSA are associated with complicated skin and soft tissue infections and severe necrotizing pneumonia, as the pathogen breaks down host epithelial tissue barriers (Lim et al., 2012; Wang et al., 2007). We tested the effect of micromolar

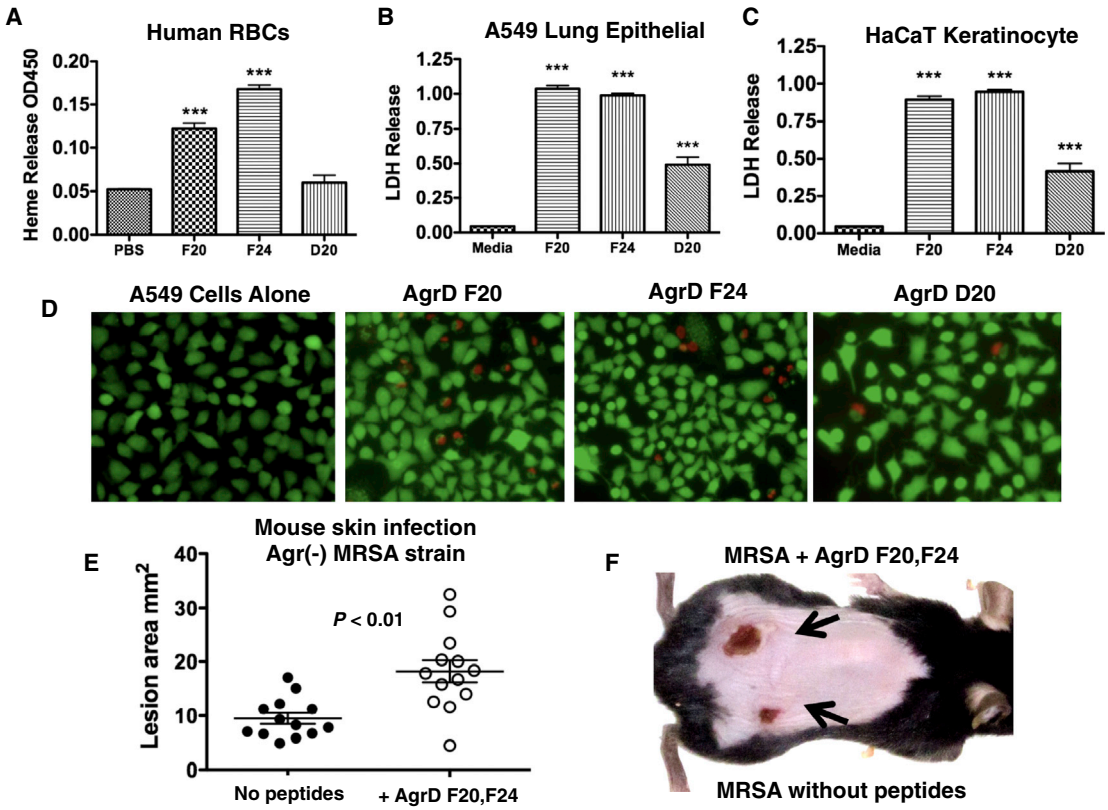

Figure 3. Erythrocyte Hemolysis, Cytotoxic Properties of N-AgrD against Epithelial Cells, and Murine Models of Infection

(A) Heparinized human whole blood was processed and treated with N-ArgD peptides or saline control. N-AgrD F20 and N-AgrD F24 showed moderate hemolysis activity. The N-AgrD D20 peptide did not cause hemolysis.

(B and C) A549 human alveolar epithelial cell (B) and HaCaT human keratinocyte cell lines (C) were incubated with N-AgrD peptides for 120 min; cell damage was monitored by LDH release. All three peptides displayed significant cytolytic activity. Statistical analysis by one-way ANOVA; ***$p < 0.001$.

(D) Fluorescent microscopy of A549 cells after live/dead cell staining.

(E) In vivo contribution of the N-AgrD F20 and N-AgrD F24 peptides as assessed in murine lesion infection models. Subcutaneous infection of C57Bl/6 mice with an *S. aureus* agr null strain was tested with and without the addition of a 1:1 mixture of AgrD F20 and AgrD F24 (10 μg/ml) on contralateral flanks. Statistical analysis was performed by Student's t test; **$p < 0.01$.

(F) Appearance of a representative infected mouse flank shows that addition of the N-AgrD F20 + N-AgrD F24 peptides to the *S. aureus* agr null strain results in an approximate doubling of lesion area.

All statistical data are expressed as mean ± SD.

concentrations of N-AgrD peptides on a human alveolar epithelial cell line (A549) and a human keratinocyte cell line (HaCaT). As measured by lactate dehydrogenase (LDH) release, N-AgrD F20 and N-AgrD F24 formylated peptides exhibited twice the cytolytic activity against both tissue cell lines as the nonformylated N-AgrD peptide (Figures 3B and 3C). A549 and HaCaT cytotoxicity was corroborated by live/dead cell counts (Figures S7A and S7B) and visual assessment by microscopy (Figure 3D; Figure S7C). Additionally, a scrambled-sequence peptide was included as a negative control and showed no activity, verifying that N-AgrD bioactivity is sequence-specific.

N-AgrD Peptides Aggravate Skin Lesions in a Murine Model

S. aureus is the most common cause of skin and soft tissue infections in humans, and the majority of the isolates cultured from these infections are predominately *agr* positive. We sought to determine the contribution of N-AgrD peptides to disease progression in vivo independent of the well-established role of the Agr system in virulence. To that end, we inoculated mice subcutaneously with the *agr* null strain *S. aureus* RN6911 in the presence or absence of a micromolar mixture of the N-AgrD F20 and N-AgrD F24. Presence of the N-AgrD peptides significantly increased ensuing lesion sizes (Figure 3E). After 72 hr, the lesion sizes caused by the RN6911 strain harvesting the N-AgrD peptides were approximately double in size (Figures 3E and 3F) despite equal bacterial loads (Figure S8), consistent with the endogenous proinflammatory and cytotoxic properties of these peptides observed in our in vitro testing. Permission to undertake experiments was obtained from the Animal Subject Ethics Committee of the University of California, San Diego.

DISCUSSION

The current functional assignment for the N-terminal region of AgrD indicates the amphipathic peptide governs intercellular

membrane anchoring and successive processing by AgrB (Zhang et al., 2004). Our study shows the extracellular release of N-AgrD as a set of bioactive structurally diverse peptides, including formylated variants. These findings indicate that *S. aureus* has evolved to maximize or chemically salvage its protein repertoire in order to gain ecological fitness.

N-AgrD structurally resembles the PSM toxin family in *S. aureus*. PSMs are cytolytic, formylated and nonformylated peptide variants that are upregulated in community-associated MRSA and genetically linked to the *agr* system (PSMγ is embedded within RNAIII) (Wang et al., 2007; Gonzalez et al., 2014). Because of the structural similarities between peptides, N-AgrD could play a potential role in biofilm structural formation as demonstrated for PSMs (Periasamy et al., 2012). In concurrence with the work herein, N-AgrD was recently shown to be a constituent of amyloid fibrils of biofilms and possess further cellular functions akin to PSMs (Schwartz et al., 2014).

Mechanisms governing the amounts of N-AgrD participating in amyloid fibrils (biofilm) versus free to the surrounding environment is likely a dynamic process governed by environmental stimuli. This notion is supported by our observation that subinhibitory concentrations of cell-wall inhibiting antibiotics or LL-37 increased abundance of N-AgrD peptides in a similar manner to PSMs (Gonzalez et al., 2012). The interplay between promiscuous *S. aureus* exoproteases and the AgrD leader domain may lead to the wide repertoire of N-AgrD variants. Proteolysis studies on the AIP showed *S. aureus* supernatants produced variant cleavage products of the N-terminal AgrD domain independent of SpsB (Kavanaugh et al., 2007). Our accumulated studies on the AgrD leader domain show unforeseen, yet important components of the now classical *agr* pathway.

In summary, we applied MS-based tools to identify N-AgrD variants that possess cytotoxic and proinflammatory activities. These peptides potentially modulate *S. aureus* disease manifestations, and suggest that the N-terminal leader domain of this protein is not simply an innocuous castoff during processing of the mature AIP. Like many pattern recognition molecules with mixed proinflammatory and toxic activities, their effect on the host is complex and likely to vary dependent on the site, stage, and magnitude of infection. Therefore, the effects N-AgrD variants have on *S. aureus* gene regulation (i.e., AgrA-AgrC signaling) merits further study. Ultimately, this work exemplifies the use of an emerging tool like molecular networking can aid in elucidating molecules that influence the establishment of infection, leading to better understanding their broader impact on the pathogen-host interaction.

SIGNIFICANCE

Our results reveal that the N-terminal leader end of the AIP substrate AgrD is an extracellularly released peptide existing in variant forms with unexpected bioactivities in vitro and in vivo. These peptides may play a role in MRSA virulence; before this study, only the core amino acids of mature AgrD were believed to contribute to bacterium's pathogenic cycle. This project arose by the application of the new and emerging tool of MS-based molecular networking, which highlights the value of integrating cutting-edge analytical tools to the study of biological systems. Because the complex array of virulence factors produced by MRSA is not fully understood, it is critical to apply new strategies that extend beyond the classical paradigm of proteomic identification. These new technologies can lead to unforeseen information on the molecular repertoire of human pathogens.

EXPERIMENTAL PROCEDURES

Identification of N-AgrD by MS

S. aureus cultures (Table S1) were grown in Todd-Hewitt broth at 37°C to late exponential-early stationary growth phase and pelleted at 4,000 rpm × 10 min, and 1 ml supernatant was collected, extracted with an equal volume of 1-butanol, and dried by SpeedVac. SDS-PAGE gels showed no Coomassie staining indicative of larger proteins; therefore, the extracts were considered to contain peptides and other small molecular weight species. Solid extracts were resuspended and processed by Thermo-Finnegan linear trap quadruple liquid chromatography tandem MS. Peptidogenomic annotation of the collected tandem MS data indicated sequence tags of the N-AgrD, and mass offsets of +28 Da were localized to the N-terminal methionine residue. Targeted use of the MS processing program InsPecT identified several N-AgrD variant peptides with formylated initiator methionine residues. Here we focused on the three most abundant and highest scoring peptides obtained from InsPecT, after validation of the assignments by manual annotation.

Synthetic Peptides

The following peptides were synthesized by American Peptide: (1) N-AgrD F20: formyl-MNTLFNLFFDFITGILKNIG; (2) N-AgrD F24: formyl-MNTLFNLFFDFITGILKNIGNIAA; (3) N-AgrD D20: FNLFFDFITGILKNIGNIAA; and (4) scramble peptide N-AgrD D20: NIAKFFLTIILFNNDFGAGI. Additional experimental procedures can be found in Supplemental Experimental Procedures.

SUPPLEMENTAL INFORMATION

Supplemental Information includes Supplemental Experimental Procedures, three figures, and one table and can be found with this article online at http://dx.doi.org/10.1016/j.chembiol.2014.09.015.

ACKNOWLEDGMENTS

D.J.G. was supported through fellowships from the A.P. Giannini Medical Research Foundation, the UC President's Postdoctoral Fellowship Program, and the University of California, San Diego, NIH International Research and Academic Career Development K12 program (GM068524). Research was supported by NIH grants HD071600 (V.N.), AI057153 (V.N.), GM097509 (P.C.D.), and GMS10RR029121 (P.C.D.). The MS data are deposited in GNPS-MASSIVE (http://gnps.ucsd.edu). We thank Jack E. Dixon for allowing access to analytical instrumentation used to generate data in this study.

Received: June 9, 2014
Revised: August 28, 2014
Accepted: September 2, 2014
Published: November 6, 2014

REFERENCES

Abdelnour, A., Arvidson, S., Bremell, T., Rydén, C., and Tarkowski, A. (1993). The accessory gene regulator (*agr*) controls *Staphylococcus aureus* virulence in a murine arthritis model. Infect. Immun. *61*, 3879–3885.

Brinkmann, V., Reichard, U., Goosmann, C., Fauler, B., Uhlemann, Y., Weiss, D.S., Weinrauch, Y., and Zychlinsky, A. (2004). Neutrophil extracellular traps kill bacteria. Science *303*, 1532–1535.

Dixit, N., Kim, M.H., Rossaint, J., Yamayoshi, I., Zarbock, A., and Simon, S.I. (2012). Leukocyte function antigen-1, kindlin-3, and calcium flux orchestrate neutrophil recruitment during inflammation. J. Immunol. *189*, 5954–5964.

Enright, M.C., Robinson, D.A., Randle, G., Feil, E.J., Grundmann, H., and Spratt, B.G. (2002). The evolutionary history of methicillin-resistant *Staphylococcus aureus* (MRSA). Proc. Natl. Acad. Sci. U S A *99*, 7687–7692.

Gonzalez, D.J., Okumura, C.Y., Hollands, A., Kersten, R., Akong-Moore, K., Pence, M.A., Malone, C.L., Derieux, J., Moore, B.S., Horswill, A.R., et al. (2012). Novel phenol-soluble modulin derivatives in community-associated methicillin-resistant *Staphylococcus aureus* identified through imaging mass spectrometry. J. Biol. Chem. *287*, 13889–13898.

Gonzalez, D.J., Vuong, L., Gonzalez, I.S., Keller, N., McGrosso, D., Hwang, J.H., Hung, J., Zinkernagel, A., Dixon, J.E., Dorrestein, P.C., and Nizet, V. (2014). Phenol soluble modulin (PSM) variants of community-associated methicillin-resistant *Staphylococcus aureus* (MRSA) captured using mass spectrometry-based molecular networking. Mol. Cell. Proteomics *13*, 1262–1272.

Harraghy, N., Kerdudou, S., and Herrmann, M. (2007). Quorum-sensing systems in staphylococci as therapeutic targets. Anal. Bioanal. Chem. *387*, 437–444.

Huang, T.W., Chen, F.J., Miu, W.C., Liao, T.L., Lin, A.C., Huang, I.W., Wu, K.M., Tsai, S.F., Chen, Y.T., and Lauderdale, T.L. (2012). Complete genome sequence of *Staphylococcus aureus* M013, a pvl-positive, ST59-SCCmec type V strain isolated in Taiwan. J. Bacteriol. *194*, 1256–1257.

Junio, H.A., Todd, D.A., Ettefagh, K.A., Ehrmann, B.M., Kavanaugh, J.S., Horswill, A.R., and Cech, N.B. (2013). Quantitative analysis of autoinducing peptide I (AIP-I) from *Staphylococcus aureus* cultures using ultrahigh performance liquid chromatography-high resolving power mass spectrometry. J. Chromatogr. B Analyt. Technol. Biomed. Life Sci. *930*, 7–12.

Kavanaugh, J.S., Thoendel, M., and Horswill, A.R. (2007). A role for type I signal peptidase in *Staphylococcus aureus* quorum sensing. Mol. Microbiol. *65*, 780–798.

Kennedy, A.D., Porcella, S.F., Martens, C., Whitney, A.R., Braughton, K.R., Chen, L., Craig, C.T., Tenover, F.C., Kreiswirth, B.N., Musser, J.M., and DeLeo, F.R. (2010). Complete nucleotide sequence analysis of plasmids in strains of *Staphylococcus aureus* clone USA300 reveals a high level of identity among isolates with closely related core genome sequences. J. Clin. Microbiol. *48*, 4504–4511.

Kersten, R.D., Yang, Y.L., Xu, Y., Cimermancic, P., Nam, S.J., Fenical, W., Fischbach, M.A., Moore, B.S., and Dorrestein, P.C. (2011). A mass spectrometry-guided genome mining approach for natural product peptidogenomics. Nat. Chem. Biol. *7*, 794–802.

Kretschmer, D., Gleske, A.K., Rautenberg, M., Wang, R., Köberle, M., Bohn, E., Schöneberg, T., Rabiet, M.J., Boulay, F., Klebanoff, S.J., et al. (2010). Human formyl peptide receptor 2 senses highly pathogenic *Staphylococcus aureus*. Cell Host Microbe *7*, 463–473.

Lim, W.H., Lien, R., Huang, Y.C., Lee, W.J., and Lai, J.Y. (2012). Community-associated methicillin-resistant Staphylococcus aureus necrotizing pneumonia in a healthy neonate. J Microbiol. Immunol. Infect. Published online November 19, 2012. http://dx.doi.org/10.1016/j.jmii.2012.07.001.

McIlwain, S., Mathews, M., Bereman, M.S., Rubel, E.W., MacCoss, M.J., and Noble, W.S. (2012). Estimating relative abundances of proteins from shotgun proteomics data. BMC Bioinformatics *13*, 308.

Mogensen, T.H. (2009). Pathogen recognition and inflammatory signaling in innate immune defenses. Clin. Microbiol. Rev. *22*, 240–273.

Novick, R.P., Ross, H.F., Projan, S.J., Kornblum, J., Kreiswirth, B., and Moghazeh, S. (1993). Synthesis of staphylococcal virulence factors is controlled by a regulatory RNA molecule. EMBO J. *12*, 3967–3975.

Periasamy, S., Joo, H.S., Duong, A.C., Bach, T.H., Tan, V.Y., Chatterjee, S.S., Cheung, G.Y., and Otto, M. (2012). How *Staphylococcus aureus* biofilms develop their characteristic structure. Proc. Natl. Acad. Sci. U S A *109*, 1281–1286.

Pragman, A.A., and Schlievert, P.M. (2004). Virulence regulation in *Staphylococcus aureus*: the need for *in vivo* analysis of virulence factor regulation. FEMS Immunol. Med. Microbiol. *42*, 147–154.

Recsei, P., Kreiswirth, B., O'Reilly, M., Schlievert, P., Gruss, A., and Novick, R.P. (1986). Regulation of exoprotein gene expression in Staphylococcus aureus by agar. Mol. Gen. Genet. *202*, 58–61.

Schwartz, K., Sekedat, M.D., Syed, A.K., O'Hara, B., Payne, D.E., Lamb, A., and Boles, B.R. (2014). The AgrD N-terminal leader peptide of Staphylococcus aureus has cytolytic and amyloidogenic properties *82*, 3837–3844.

Tanner, S., Shu, H., Frank, A., Wang, L.C., Zandi, E., Mumby, M., Pevzner, P.A., and Bafna, V. (2005). InsPecT: identification of posttranslationally modified peptides from tandem mass spectra. Anal. Chem. *77*, 4626–4639.

Thoendel, M., and Horswill, A.R. (2009). Identification of *Staphylococcus aureus* AgrD residues required for autoinducing peptide biosynthesis. J. Biol. Chem. *284*, 21828–21838.

Villaruz, A.E., Bubeck Wardenburg, J., Khan, B.A., Whitney, A.R., Sturdevant, D.E., Gardner, D.J., DeLeo, F.R., and Otto, M. (2009). A point mutation in the *agr* locus rather than expression of the Panton-Valentine leukocidin caused previously reported phenotypes in *Staphylococcus aureus* pneumonia and gene regulation. J. Infect. Dis. *200*, 724–734.

Wang, R., Braughton, K.R., Kretschmer, D., Bach, T.H., Queck, S.Y., Li, M., Kennedy, A.D., Dorward, D.W., Klebanoff, S.J., Peschel, A., et al. (2007). Identification of novel cytolytic peptides as key virulence determinants for community-associated MRSA. Nat. Med. *13*, 1510–1514.

Watrous, J., Roach, P., Alexandrov, T., Heath, B.S., Yang, J.Y., Kersten, R.D., van der Voort, M., Pogliano, K., Gross, H., Raaijmakers, J.M., et al. (2012). Mass spectral molecular networking of living microbial colonies. Proc. Natl. Acad. Sci. U S A *109*, E1743–E1752.

Wright, J.S., 3rd, Traber, K.E., Corrigan, R., Benson, S.A., Musser, J.M., and Novick, R.P. (2005). The *agr* radiation: an early event in the evolution of staphylococci. J. Bacteriol. *187*, 5585–5594.

Zhang, L., Lin, J., Ji, G. (2004) Membrane anchoring of the AgrD N-terminal amphipathic region is required for its processing to produce a quorum-sensing pheromone in Staphylococcus aureus. *279*, 19448–19456.

Chemistry & Biology, Volume *21*

Supplemental Information

N-Terminal ArgD Peptides from the Classical *Staphylococcus aureus* Agr System Have Cytotoxic and Proinflammatory Activities

David J. Gonzalez, Ross Corriden, Kathryn Akong-Moore, Joshua Olson, Pieter C. Dorrestein, and Victor Nizet

SUPPLEMENTAL INFORMATION

Functional Properties of N-Terminal ArgD Peptides from the Classical *Staphylococcus aureus* Agr System

David J. Gonzalez[1,2], Ross Corriden[3], Kathryn Akong-Moore[3], Joshua Olson[3], Pieter C. Dorrestein[1,2,4] and Victor Nizet[2,3]

[1]Department of Pharmacology, University of California, San Diego, La Jolla, CA 92093, USA
[2]Skaggs School of Pharmacy and Pharmaceutical Sciences, University of California, San Diego, La Jolla, CA 92093, USA
[3]Department of Pediatrics, University of California, San Diego, La Jolla, CA 92093, USA
[4]Department of Chemistry and Biochemistry, University of California, San Diego, La Jolla, CA 92093, USA

Content **Page**

Staphylococcus aureus Strain	Agr Type	Predicted Clonal Colony Type	AgrD MS ID
Clinical Isolate 03	1	8	Yes
Clinical Isolate 08	1	8	Yes
Clinical Isolate 42	1	8	No
Clinical Isolate 44	1	45	No
Clinical Isolate 61	1	59	Yes
Clinical Isolate 79	1	45	Yes
JH1	2	5	No
RN9120 (Agr null)	2	na	No
Mu50	na	5	No
Sanger 252	3	36	No
Clinical Isolate 59	1	59	Yes
TCH1516	1	8	Yes

Supplemental Table S1, related to Figure 1. *Staphylococcus aureus* strains in AgrD peptide screen. A search for *Staphylococcus aureus* strains that released detectable quantities of N-terminal AgrD peptides was expanded to 12 isolates including several clinically derived strains. Among these 12 isolates AgrD peptides were detectable in five strains in three USA300 lineage MRSA, TCH1516 and two designated sequence type (ST) 8, a ST59 MRSA or commonly known as the Taiwan clone, and clonal colony ST45 of USA600 MRSA lineage.

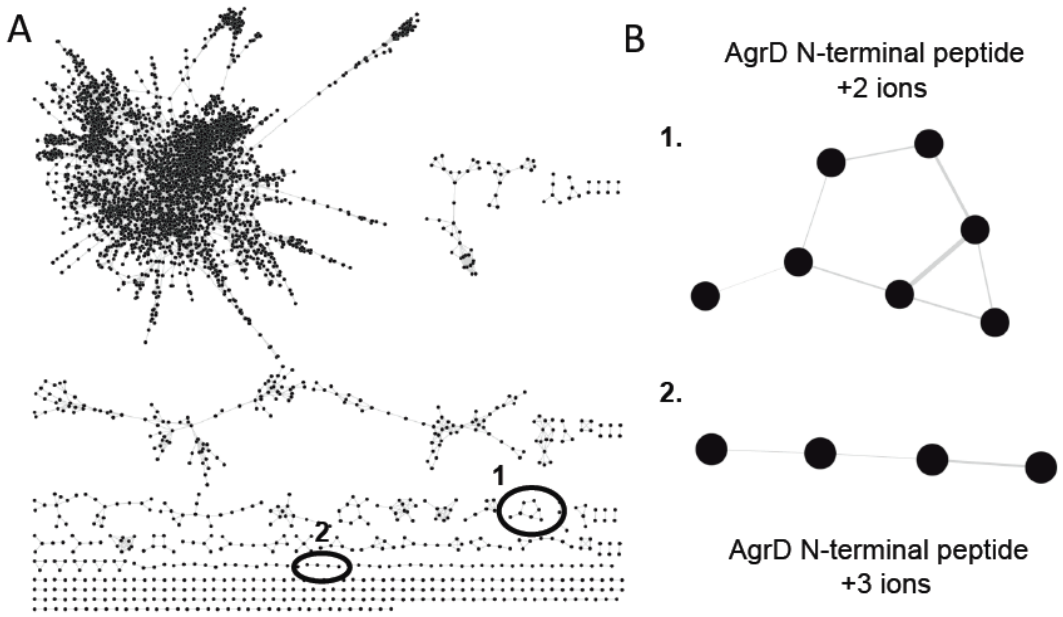

Supplemental Figure S1, related to Figure 1. *S. aureus* TCH1516 molecular network map. **(a)** Complete Molecular Network map constructed from *Staphylococcus aureus* USA300 strain TCH1516 peptides and small molecules. Media components and mass spectrometry solvent-derived ions were subtracted from the network. **(b)** Cluster 1 shows a node cluster identified through sequencing to originate from the N-terminal region of the AgrD peptide substrate. Cluster 1 was composed of +2 charged ions. It was also determined that Cluster 2 originated from the N-terminal region of AgrD and was composed of +3 ion pairs.

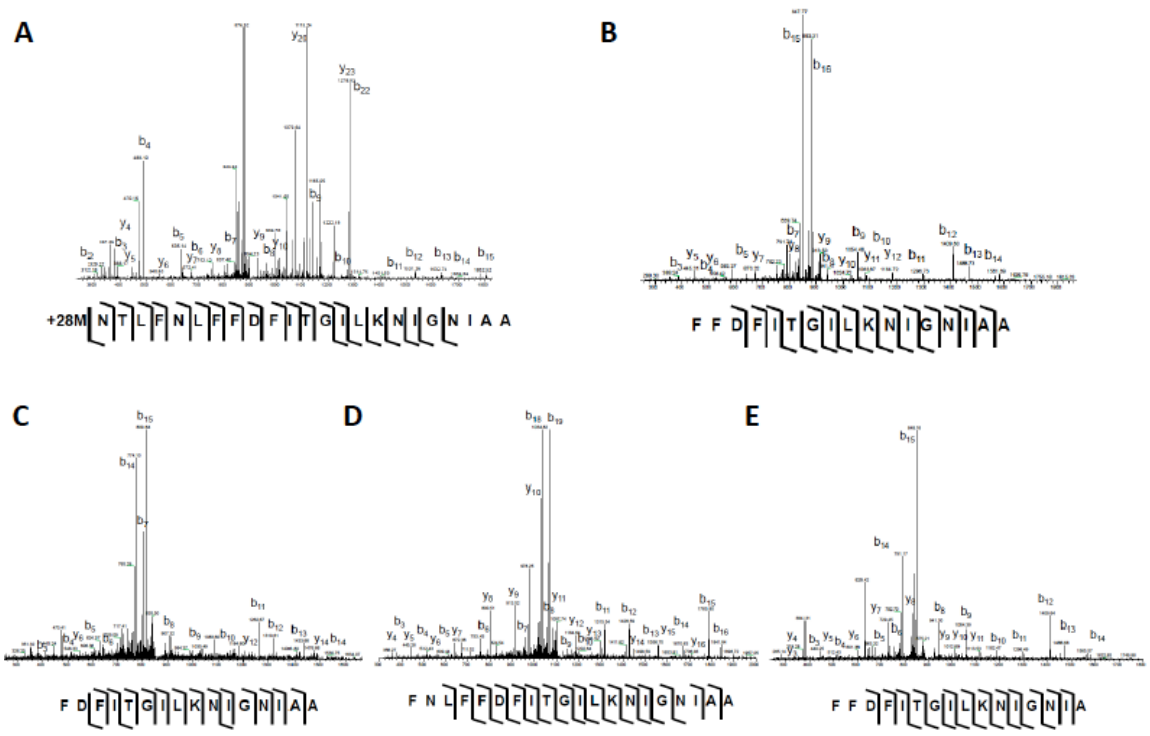

Supplemental Figure S2, related to Figure 1. Tandem MS for identified AgrD N-terminal variants. The parent ion for each displayed peptide in was isolated within the mass spectrometer and fragmented using collision-induced dissociation. Ions corresponding to fragmentations at the peptide bond are indicated as b (N-terminal coverage) or y (C-terminal coverage) and so labeled. **A.** Tandem mass spectrum for the peptide formylated AgrD F24. **B.** Tandem mass spectrum for non-formylated AgrD D17. **C.** Tandem mass spectrum for the peptide non-formylated AgrD D16. **D.** Tandem mass spectrum for the peptide non-formylated AgrD D20. **E.** Tandem mass spectrum for the peptide non-formylated AgrD D16B.

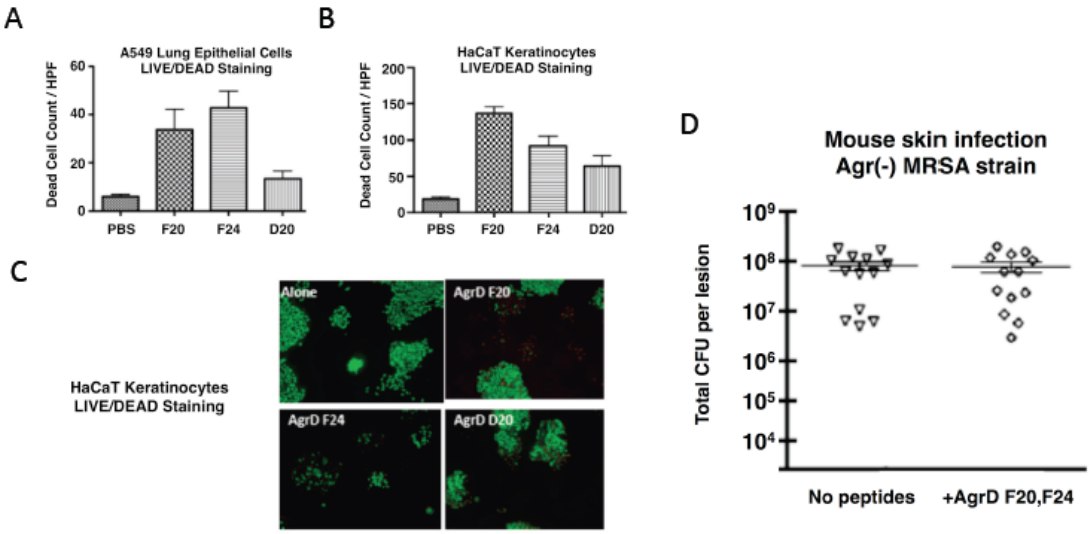

Supplemental Figure S3, related to Figure 3. Cytotoxicity, hemolysis and murine skin lesion colony forming unit counts. A549 and HaCaT LIVE/DEAD cell counts after incubation with the AgrD peptides. **(a)** A549 cells were incubated with 10 µg/µl of the indicated AgrD peptides. Thereafter, cells were stained using the Invitrogen LIVE/DEAD cell viability kit and counted under microscopy through four random fields of view. **(b)** HaCaT cells were incubated with 10 µg/µl of the indicated AgrD peptides. Thereafter, cells were stained with the Invitrogen LIVE/DEAD cell viability kit and counted under microscopy through four random fields of view. **(c)** HaCaT cells stained with LIVE/DEAD fluorescent dyes. Red dye is indicative of damaged cells and green stain is indicative of viable cells. A larger number of non-viable cells were observed post-incubation with the AgrD peptides compared to the untreated control. **(d)** Addition of AgrD F20 and AgrD F24 peptides do not alter *Staphylococcus aureus* survival in a skin lesion model. Subcutaneous infection of C57Bl/6 mice with an *S. aureus agr* null strain was tested +/- addition of a 1:1 mixture of AgrD F20 and AgrD F24 (10 µg/ml) on contralateral flanks; each mouse served as its own control. Statistical analysis was performed by Student's T-test; nonsignificant. This contrasts with increased lesion size associated with AgrD peptide treatment.

Supplemental Materials and Methods

Neutrophil chemotaxis

Human neutrophils were isolated by Polymorph Prep kit per manufacturer's instructions. Neutrophil migration was quantified by a previously reported transwell assay[1]. Briefly, either fMLP (Sigma Aldrich, MO) or formylated peptides in HBSS were placed in the lower wells (650 µl total volume, 385 nM final peptide concentration) of a 24-well Transwell plate with 3 µm pore size (Corning). A total of 1 x 10^7 cells in 150 µl of Hank's buffered saline solution (HBSS) were placed in the upper chambers, and plates incubated at 37˚C for 30 min with 5% CO2 to allow cell migration. Cells entering the lower chambers were lysed by adding 130 µl 0.5% Triton X-100 (pH 7.4) for 10 min. Elastase activity, a measure of relative cell migration to the lower wells, was quantified by adding 1 mM (final concentration) p-nitroanilide (Sigma Aldrich, MO) for 30 min and absorbance at 405 nm using a SpectraMax M3 plate reader (Molecular Devices, CA).

Neutrophil calcium flux

Calcium fluxes in human neutrophil were measured as described [2], with minor modifications. Briefly, neutrophils were incubated with 2 µM Fluo-3 in PBS at 37˚C for 30 min. After a 5 min spin at 300 g, cells were resuspended in PBS at 1 x 10^6 cells/ml. Prior to the assay, cell preparations were either left untreated or pre-incubated with 10 µM final concentration of BOC-MLF or PBP10 (both obtained from Tocris, UK), antagonists of FPR1 and FPR2, respectively. Samples (500 µl) were transferred to 5 ml polystyrene round bottom tubes and analyzed by flow cytometry before and after addition

of formylated peptides (385 nM final concentration) while vortexing. A total of 3000 events were recorded, and resulting data analyzed by gating for the neutrophil population and measuring geometric mean fluorescence intensity (gMFI) using FloJo (Tree Star, OR) software. Data are expressed as gMFI relative to untreated cells.

Neutrophil extracellular traps (NETs)

Neutrophils were added at 2 x 105 cells/well in RPMI media a 48-well tissue culture plate. Phorbol 12-myristate 13-acetate (PMA) stimulation (25 nM) was used as a positive control. AgrD peptides were incubated for 180 min at 10 μg/ml. Thereafter, 500 mU of micrococcal nuclease were added for 10 min and the reaction halted with 5 mM EDTA. The plate was centrifuged and supernatants analyzed by the Quant-iT Picogreen (Invitrogen) assay per manufacturer's instructions. For microscopic confirmation, neutrophils were placed on poly-L-lysine-coated glass slides, treated with AgrD peptides or vehicle controls, and NETs visualized using a rabbit antimyeloperoxidase antibody followed by a secondary goat anti-rabbit Alexa 488 antibody; samples were embedded in 4,6-diamidino-2-phenylindole (DAPI) to counterstain DNA in blue. Mounted samples were examined using an inverted confocal laser-scanning two-photon microscope, Olympus Fluoview FV1000.

AgrD peptide cytotoxicity assays

A549 adenocarcinomic human alveolar epithelial cells or HaCaT keratinocytes were maintained in a 5% CO2, water-saturated atmosphere at 37°C in DMEM (Gibco). Cells were grown to 70–90% confluence in 24-well microtiter plates, washed and treated with

10 μg/mL of AgrD F20, AgrD F24 and AgrD D20 for 4 h. Culture supernatants were prepared for the Promega CytoTox 96 non-radioactive cytotoxicity assay kit per manufacturer's instructions and absorbance at 490 nm recorded.

AgrD peptide hemolysis assay

Defibrinated sheep blood or human blood was washed in PBS and diluted to a final concentration of 1:25 (v/v). Washed blood was placed in individual wells of a flat-bottom 96-well microtiter plate (Costar, Corning). AgrD peptides at 10 μg/ml were added directly to the wells, and the mixture was incubated for 4 h at 37°C. After incubation, plates were centrifuged at 500 x *g* for 5 min, and an aliquot of supernatant placed in a separate microtiter plate to measure hemoglobin absorbance at 450 nm on a microplate reader.

AgrD murine skin infection model

Permission to undertake experiments was obtained from the Animal Subject Ethics Committee of the University of California, San Diego. Flanks of 9 week old female C57 mice (n = 12) were shaved and naired. The following day, mice were anaesthetized with ketamine/xylazine and contralateral flanks injected with 1 x 10^8 CFU of S. aureus RN691 (agr I null) strain in 100 μl saline in the presence or absence of a 1:1 mixture of AgrD F20 and AgrD F24100 (10 μg/mL) – each mouse serving as its own control. After 3 days, lesions were harvested using sterile surgical scissors/forceps at the lesion margin; if no lesion was present, the area at the site of injection was excised. The program ImageJ was used to calculate lesion area and expressed in millimeters squared. Statistical

analysis of the lesion areas was performed by paired T-test using the Prism software. Tissue was homogenized using a BeadBeater (Biospec) and serial dilutions plated on THB agar for enumeration of colony forming units and calculation of bacterial burden (Supplemental Figure 4).

References

1. Corriden, R. et al. Ecto-nucleoside triphosphate diphosphohydrolase 1 (E-NTPDase1/CD39) regulates neutrophil chemotaxis by hydrolyzing released ATP to adenosine. *J Biol Chem* **283**, 28480-6 (2008).
2. Veldkamp, K.E., Heezius, H.C., Verhoef, J., van Strijp, J.A. & van Kessel, K.P. Modulation of neutrophil chemokine receptors by *Staphylococcus aureus* supernate. *Infect Immun* **68**, 5908-13 (2000).